

# The Possibility of Utilizing the Composite Ferrites as Core Material for the Fabrication of Multilayer Chip Inductors

Varalaxmi N\*

Department of Physics, University College, Kakatiya University, Warangal, India

## Abstract

This work mainly focuses on the investigation carried out on MgCuZn and NiCuZn ferrites which are widely employed for many electronic applications, they are very promising candidate for microinductor applications particularly to produce multilayer chip inductors (MLCIs) due to their excellent properties. Ferrite composites powder of  $Mg_{0.6}Cu_{0.1}Zn_{0.4}Fe_2O_4$  and  $Ni_{0.35}Cu_{0.05}Zn_{0.6}Fe_2O_4$  powder were synthesized by conventional ceramic double sintering technique. After being mixed with different volume fractions, a series of novel and dense composites with generic formula  $(1-X)Mg_{0.6}Cu_{0.1}Zn_{0.4}Fe_2O_4 + (X)Ni_{0.35}Cu_{0.05}Zn_{0.6}Fe_2O_4$  were obtained in which X varies from 0.0 to 1.0. The presence of phases was confirmed by X-ray diffraction studies which confirms the formation of single phase cubic spinel structure and the grain size was estimated using SEM micrographs. In search of the suitable ferrite materials for microinductor applications, assuming that the ferrite composites would yield enhanced magnetic properties, an investigation is carried out on the composite ferrites and on the pure. To investigate the magnetic and electrical properties which studies were carried out in the temperature range 30 to 360°C and within the frequency range 100 Hz to 1MHz. These studies revealed that these ferrites possess good electromagnetic properties and can be exploited as core material for microinductor applications.

**Keywords:** Nano composites • Magnetic properties • Electrical Properties • Microinductor Applications • Multilayer layer chip inductors

## Introduction

Nanotechnology is a fast-growing area, involving the fabrication and use of nano-sized materials and devices. Various nanocomposite materials play a significant important roles in modern science and technology. Many nanocomposites of different varieties have been developed over recent years. There is a great need and demand for these materials.

As the composite materials have an important industry and technological role, because the composites have interesting properties, which could be achieved either of the constituent material alone, also exhibiting simultaneously significant properties have been of great interest to modern science and technology, not only from the viewpoint of solid state physics, but also, because of their potential for practical applications in electronic devices and systems [1-6]. The rapid evolution of high-speed digital electronics, wireless communications, industrial, exposure to necessitate the electronic devices with miniaturization size, high efficiency and low cost [7]. Multilayer chip inductor (MLCI) is a passive surface mounting device (SMD) which demands the electronic components in a miniature form. Recently surface mounting devices (SMDs) are rapidly developing for electronic applications such as microinductors, also a widely used components in various electronic circuits that help greatly in the miniaturization of many latest electronic gadgets, including mobile phones, notebook computers and personal wireless communication systems. The chip inductors are fabricated by laying alternate layers of soft ferrite and silver electrodes. Better magnetic properties, especially required high initial permeability for reducing the number of layers of multilayer chip inductors (MLCIs) minimizing the capacity between the layers and realizing the miniaturization [8].

NiCuZn and MgCuZn ferrites [9-11] possess a unique combination

of wide range applications such as high frequency response, high initial permeability, Stress insensitivity, high resistivity, fairly high Curie transition temperature, environmental stability, low magnetostriction constant and MgCuZn mainly due to its low cost [8,12-15]. It is believed that increase of initial permeability can be obtained by decreasing magnetostriction constant [8,12]. As the magnetostriction constant of MgCuZn ferrite is lower than that of NiCuZn ferrite [9], it is also expected that the multilayer chip inductor (MLCIs) using MgCuZn ferrites [8] would show higher magnetic properties [12,16] making further miniaturization possible than that of NiCuZn ferrites, compared one can realize at low cost MLCIs with MgCuZn ferrites. These properties attracted for developing suitable ferrite materials for microinductor applications, two compounds can successfully incorporate into single composite expecting that the ferrite composites would yield enhanced magnetic properties, in the present investigation composite ferrites with the NiCuZn and MgCuZn ferrites as pure components were prepared along with NiCuZn-MgCuZn ferrite composites viz.,  $(1-X)Mg_{0.6}Cu_{0.1}Zn_{0.3}Fe_2O_4 + (X)Ni_{0.35}Cu_{0.05}Zn_{0.6}Fe_2O_4$  (where X varies from 0.0 to 1.0) with a view to examine whether there would be any enhancement of magnetic properties in this system, as the initial permeability of a ferrite is the most sensitive property to external stress.

Pure  $Ni_{0.35}Cu_{0.05}Zn_{0.6}Fe_2O_4$  showed excellent magnetic, electrical and stress insensitivity properties which are useful for microinductor applications [17], keeping this in view, with slight variation in NiCuZn compositions, pure  $Mg_{0.6}Cu_{0.1}Zn_{0.3}Fe_2O_4$  ferrite is choosed with an intention of preparing a composite ferrite and to investigate the behavior, for their wide range of applications, to use them as core magnetic materials for microinductor applications and the results are reported in this paper.

## Experimental Section

### Materials and methods

The ferrite composites with ferromagnetic phases have been prepared by employing conventional ceramic method. The ferrimagnetic phases MgCuZn and NiCuZn ferrites with respective compositions chosen was  $Mg_{0.6}Cu_{0.1}Zn_{0.4}Fe_2O_4$  and  $Ni_{0.35}Cu_{0.05}Zn_{0.6}Fe_2O_4$ . Stoichiometric proportions of analytical grade NiO, MgO, CuO, ZnO and  $Fe_2O_3$  were intimately mixed and resulting powders were ball milled for 40h in Restch PM 200 planetary ball mill in aqueous medium. The slurry was dried and the powders were

\*Address for Correspondence: Hussein SA Golicha, Department of Natural sciences, Garissa University, P.O. Box 1801-70100 Garissa, Kenya, Tel: 254722269849; E-mail: golicha2000@gmail.com

**Copyright:** © 2020 Golicha SA, et al. This is an open-access article distributed under the terms of the Creative Commons Attribution License, which permits unrestricted use, distribution, and reproduction in any medium, provided the original author and source are credited.

presintered at 800°C in the form of cakes. After pre-sintering, these cakes were crushed, ball-milled once again to obtain fine particle size and finally these powders were sieved to get uniform particle size. The green powder thus obtained was then pressed using a suitable die in the form of toroids and pellets

All the other details of material preparation and characterization were discussed [18].

**Experimental details**

The initial permeability ( $\mu_r$ ) data of these ferrite toroids were evaluated from the inductance measurements carried out at 1 kHz using LCR Hi-Tester (Hioki Model 3532-50, Japan) in the temperature range from 30 °C to 250 °C using the formula [18]. DC electrical conductivity measurements were carried out with laboratory designed cell having guard ring facility in addition to the two probe method [19]. The details of the instrument and Conductivity measurements are given in [20]. The measurements of AC electrical conductivity were evaluated using the relation [20] and Thermo-electric power were made in the temperature region 30 to 250°C by a differential method similar to that of Reddy et.al., [21] with a few modifications which are explained [20].

**Results and Discussion**

X-ray diffractograms patterns of X=0.0, 0.5 and 1.0 ferrite samples are presented in Figure 1. Strong diffraction from the planes (220), (311),

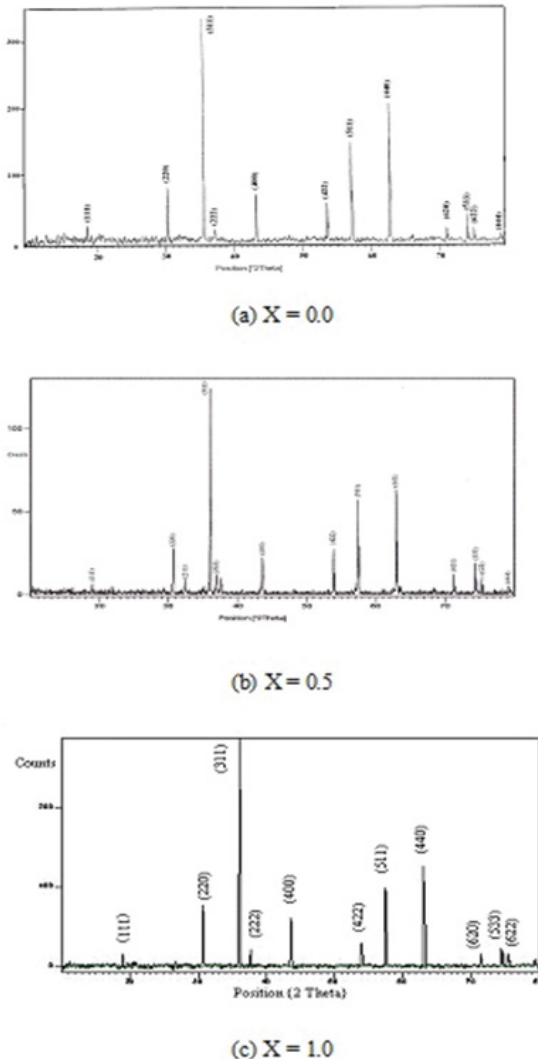
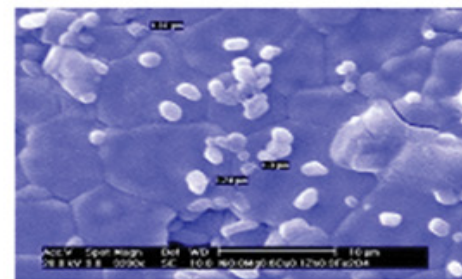


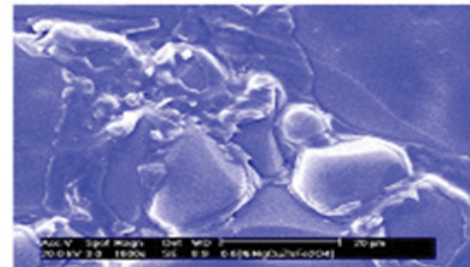
**Figure 1.** X-ray diffractograms of pure components and ferrite composite (a) X=0.0, (b) X=0.5 and (c) X=1.0.

(400), (511) and (440) as well as a weak diffraction from the planes (222) and (422) are the evidence of the formation of single phase cubic spinel structure in the both ferrites. No second phase was detected. In ferrites the planes (220), (400), (440) and (422) intensity peaks are mostly sensitive to cation distribution at both tetrahedral and octahedral sites. Generally, they depend on tetrahedral sites [22-24], whereas that of (222) peak depends on octahedral sites [22]. The intensity of the (511) peak is sensitive to oxygen content [23]. As seen from the figures, peaks in present ferrites revealed that the intensity of (422) peak got suppressed considerably. In the ferrite composite (X=0.5). Similarly the intensity of (222) peak is also reduced compared to the pure components. Hence, it can be inferred that the cation distribution is altogether different compared to the pure ferrites (X=0.0 and 1.0) of the composites. A similar report was observed [18,24]. Generally, one can observe that, for all concentrations all planes characterizing the spinel ferrite and the peak intensity depend on the concentration of magnetic ions in the lattice.

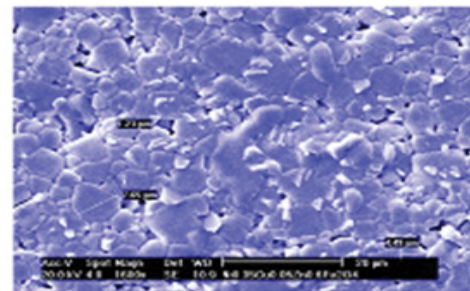
The density of the composites increases linearly with X. SEM photographs of the sintered samples were recorded to understand the microstructure of the pure and composite ferrites of X=0, 0.6 and 1.0 which are shown in Figure 2 which reveals that the grain morphologies of the pure



(a) X = 0.0



(b) X = 0.6



(c) X = 1.0

**Figure 2.** SEM photographs of ferrites composites (a) X=0.0, (b) X=0.6 and (c) X=1.0.

components and the composite (X=0.6) are different. Larger grain diameter in the samples X=0.0 and 0.6 were observed compared to X=1.0. Generally, large grained samples show high initial permeability magnitude [25]. Although the grain size is large for X=0.0 compositions, the permeability value is comparatively low. This is attributable to the porosity percentage and the presence of a number of voids indicating comparatively large grain separation causing a decrease in bulk density.

The calculated lattice parameter identified the samples to be cubic spinel. It's noticed from Table 1 which shows the variation of the lattice parameters of the investigated samples as a function of 'X' composition, it is clear that the lattice parameter exhibit continuous decrease with the increase of 'X' it can be explained on the basis of the relative ionic radius of ions [26,27]. The ionic radius of  $Mg^{2+}=0.65 \text{ \AA}$ ,  $Ni^{2+}=0.72 \text{ \AA}$ ,  $Cu^{2+}= 0.72 \text{ \AA}$  and  $Zn^{2+}=0.74 \text{ \AA}$  and  $Fe^{2+}=0.64 \text{ \AA}$  respectively, as the varying components are  $Mg_{0.6}Cu_{0.1}Zn_{0.3}Fe_2O_4$  and  $Ni_{0.35}Cu_{0.05}Zn_{0.6}Fe_2O_4$ , in which majority composition dominating is  $Mg^{2+}$ ,  $Ni^{2+}$  and  $Zn^{2+}$  though the ionic radius of  $Ni^{2+}=0.72 \text{ \AA}$  and  $Zn^{2+}=0.74 \text{ \AA}$  are larger in radius when compared to  $Mg^{2+}=0.65 \text{ \AA}$ , which has smaller radius may cause a decrease of lattice constant may be logically attributed due to the difference in the ionic radius, which results in the reduction of the unit cell. Particle sizes of as prepared ferrite powders were calculated from X-ray peak broadening of the (311) diffraction peak using the Scherrer formula [28] are found to be varying between 4 to 6  $\mu m$ . The values of the particle size, lattice constant (a) and measured density ( $\rho_m$ ) data are given in Table 1.

The magnetic properties of the soft ferrites are influenced by the compositions, additives and microstructures of the materials. Among these factors, the microstructures have great effect on magnetic properties. It is generally believed that the larger the grain sizes, the higher the saturation and initial permeability.

The initial permeability is known to be one of the most sensitive magnetic properties of ferrites. Data obtained at room temperature for various compositions of the composite ferrites along with the Curie temperature  $T_c$  are presented in Table 1. In Table 1, with increasing X, the initial permeability magnitude increases. The initial permeability values of pure ferrites are 586 and 1041 for X=0.0 and X=1.0 respectively. This behaviour of initial permeability seems to be in accordance with the densities of the samples as the maximum permeability's are recorded for samples with higher densities. It is known that ferrites with higher density and larger average grain size possess a higher initial permeability [29]. Hence, the increase in initial permeability of these composite ferrites may be primarily attributed an increase in the density, not only results in the reduction of demagnetizing field due to the presence of pores, but also raise the spin rotational contribution, which in turn increase the permeability [30]. In fact, the initial permeability of ferrite is usually expressed as follows;  $\mu = M_s^2 / (aK + b\lambda\sigma)$ ,

Where  $\mu$  is the initial permeability, M the saturation magnetization,  $\lambda$  the magnetostriction constant,  $\sigma$  the inner stress, K the crystal magnetic anisotropy, a and b are constants.

So, the major role of the increased permeability in compositions is attributed to the decrease in magnetostriction constant mainly and may

**Table 1.** The density ( $\rho$ ), Lattice parameter (a), initial permeability ( $\mu_i$ ), Particle Size and Curie temperature ( $T_c$ ) of the ferrite composite system (1-X)  $Mg_{0.6}Cu_{0.1}Zn_{0.4}Fe_2O_4$  + (X)  $i_{0.35}Cu_{0.05}Zn_{0.6}Fe_2O_4$  at RT.

S.No	Composition X	Lattice Parameter $\text{\AA}$	Density $kg.m^{-3}$	Initial permeability $\mu_i$	Curie temperature $T_c$ $^{\circ}C$	Particle Size 't' $\mu m$
1)	0.0.	8.374	4.267	585	230	5.27
2)	0.2	8.343	4.389	596	80	5.64
3)	0.4	8.327	4.641	640	120	5.71
4)	0.5	8.321	4.714	670	130	4.74
5)	0.6	8.318	4.817	706	140	5.94
6)	0.8	8.315	4.963	803	200	5.93
7)	1.0	8.314	5.568	1041	180	5.64

be in parts, decrease in the anisotropy and inner stresses in this narrow composition range. The initial permeability increases with increasing temperature. This phenomenon is attributed to the contribution of domain wall motion, The behaviour of the initial permeability ( $\mu_i$ ) as a function of temperature could explain the method for Curie temperature, it can be seen from Figure 3 that as the temperature increases continuously, the initial permeability ( $\mu_i$ ) also increases up to a certain temperature, increases to a peak value and then abruptly falls to a minimum value i.e., Zero or 1. The temperature at which this abrupt fall takes place is the magnetic Curie transition temperature ( $T_c$ ). At this temperature, the specimens transform from the ferrimagnetic phase to the paramagnetic phase. The temperature point at which initial permeability ( $\mu_i$ ) drops down from a very high value to near a low value is called Curie temperature (or) Curie point and the initial permeability ( $\mu_i$ ) peak value just before the Curie point is reached called as "Hoppingson peak" and higher values of  $\mu_i$  appear near the Curie point.

The Frequency dependency of the permeability, measured in the frequency 100 Hz to 1MHz is shown graphically in Figure 4. The permeability is almost stable in the frequency range 100 to 10KHz and its shows dispersion above 10KHz frequency. In general, the permeability of spectra is related to two different magnetization mechanisms: spin rotation and domain wall magnetizations [31]. It is known that the high frequency dispersions are associated with domain wall dynamics [32] which may be more due to the predominance of the domain wall motion than spin rotation [33]. The increase in frequency dispersions indicates the decreases of critical field. This decrease in cutoff frequency is attributed to the increase in initial permeability following Snoek's law [34].

DC resistivity is an important property for the ferrites when utilized for MLCIs in high frequency range. The room temperature compositional dependence of DC resistivity and conductivity values of these composite ferrites are also listed in Table 2. It is so clear that the resistivity values of all

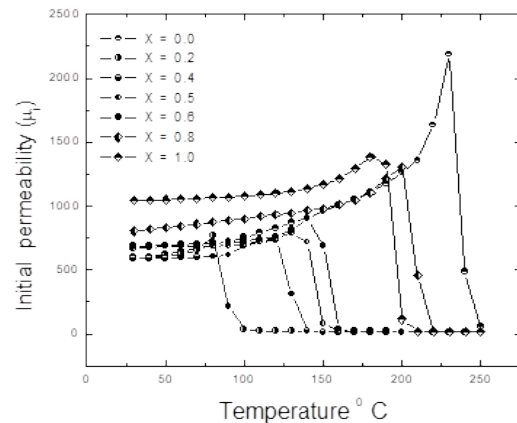


**Figure 3.** Variation of initial permeability as a function of temperature for NiCuZn-MgCuZn composite ferrites.

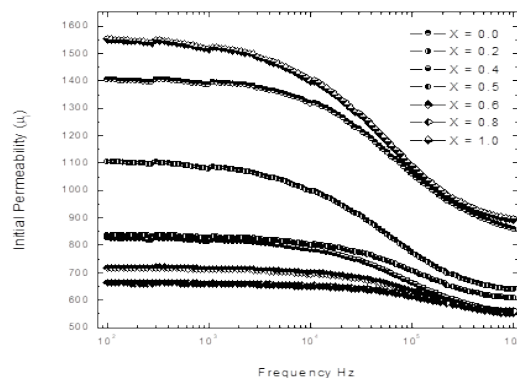


**Figure 4.** Dependence of initial permeability on frequency for NiCuZn-MgCuZn composite ferrites.



ferrites composites are found to be  $10^9 \Omega \text{ cm}$  which meets the requirement of MLCIs.

As observed from Table 2, the DC electrical resistivity ( $\rho_{DC}$ ) of the composites ferrite increases in magnitude with increasing 'X'. The conduction mechanism in ferrite is considered as the electron hopping between Fe and Fe in B site. Increasing of resistivity is may be due to the volatilization of zinc and the formation of  $\text{Fe}^{2+}$  ions supporting electron hopping between  $\text{Fe}^{2+}$  and  $\text{Fe}^{3+}$  [35]. Loss of zinc will be comparatively less. The increase of resistivity in the materials is due to electron-hole compensation as was suggested [36]. Since  $\text{MgCuZnFe}_2\text{O}_4$  is an N-type semiconductor but  $\text{NiCuZnFe}_2\text{O}_4$  is a P-type semiconductor [20], the resistivity increases with the increase of the oxidation of  $\text{Ni}^{2+}$  to  $\text{Ni}^{3+}$ . For higher zinc contents there will be smaller amounts of holes.

The variation of DC conductivity ( $\log \sigma_{DC}$ ) with reciprocal of temperature is shown in Figure 5. It can be observed from the figure that the behaviour of  $\log \sigma_{DC}$  with  $10^3/T$  shows an increasing trend with increasing temperature exhibiting a semiconductor behaviour.

The AC electrical conductivity ( $\sigma_{AC}$ ) values for various compositions of these composite ferrites obtained at room temperature are also presented in Table 2. One can observe the following, in the investigated temperature range, the conductivity decreases for various compositions. The effect of

**Table 2.** DC-AC Electrical conductivities and Seebeck coefficient composite system  $(1-X)\text{Mg}_{0.6}\text{Cu}_{0.1}\text{Zn}_{0.4}\text{Fe}_2\text{O}_4 + (X)\text{Ni}_{0.35}\text{Cu}_{0.05}\text{Zn}_{0.6}\text{Fe}_2\text{O}_4$  at RT.

S.No.	Composition	$\sigma_{DC}$ at RT $\Omega^{-1}\text{Cm}^{-1}$	$\rho_{DC}$ at RT $\Omega\text{Cm}$	$\sigma_{AC}$ at RT $\Omega^{-1}\text{Cm}^{-1}$	$\rho_{AC}$ at RT $\Omega\text{Cm}$	Seebeck Coefficient $\alpha \mu\text{S/K}$
1)	0.0.	$9.199 \times 10^{-8}$	$1.087 \times 10^7$	$1.642 \times 10^{-7}$	$6.092 \times 10^6$	-0.8
2)	0.2	$3.271 \times 10^{-10}$	$3.056 \times 10^9$	$1.213 \times 10^{-7}$	$8.246 \times 10^6$	1.2
3)	0.4	$1.890 \times 10^{-10}$	$5.290 \times 10^9$	$1.208 \times 10^{-7}$	$8.280 \times 10^6$	1.9
4)	0.5	$1.679 \times 10^{-10}$	$5.953 \times 10^9$	$1.206 \times 10^{-7}$	$8.289 \times 10^6$	2.2
5)	0.6	$1.612 \times 10^{-10}$	$6.202 \times 10^9$	$1.207 \times 10^{-7}$	$8.287 \times 10^6$	2.7
6)	0.8	$1.576 \times 10^{-10}$	$6.341 \times 10^9$	$1.215 \times 10^{-7}$	$8.229 \times 10^6$	3.2
7)	1	$1.552 \times 10^{-10}$	$6.582 \times 10^9$	$1.234 \times 10^{-7}$	$8.103 \times 10^6$	6

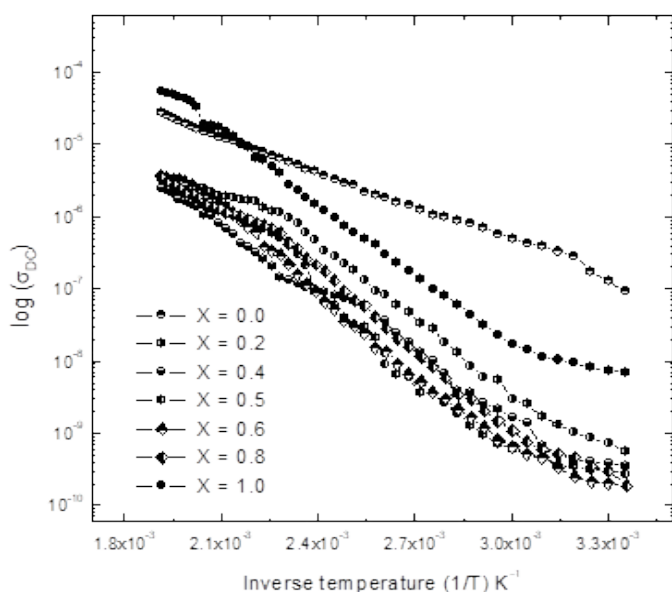


**Figure 5.** Temperature dependence of DC electrical conductivity  $\log(\sigma_{DC})$  temperature for NiCuZn- MgCuZn composite ferrites.

temperature on the AC electrical conductivity ( $\sigma_{AC}$ ) of composite ferrites were also carried out from room temperature to 360 °C. The variation of the  $\log(\sigma_{AC})$  as a function of reciprocal temperature for all the samples is plotted in Figure 6. As mentioned earlier, in DC electrical conductivity, a similar trend was observed in the case of AC electrical conductivity. The AC conductivity is found to be more in orders more than the DC electrical conductivity. The influence of temperature on conductivity can be explained by considering the mobility of charge carriers responsible for hopping.

The conduction mechanism in ferrites is generally explained based on "Polaron hopping mechanism". Polarons belong to two categories, large and small polarons. In the large Polaron model, the conductivity decreases by band mechanism at all temperatures and the AC conductivity with frequency. The small polarons conduct in band-like manner up to a certain temperature, and the conductivity shows an increase in frequency. At higher temperatures, the conduction is by thermally-activated hopping mechanism. In order to test the conduction mechanism, the variation of  $\log \sigma_{(AC-DC)}$  with  $\log \omega^2$  is observed and is shown in Figure 7. An examination of the Figure 7 reveals that  $\log \sigma_{(AC-DC)}$  versus  $\log \omega^2$  increases with increase in frequency. But at low and at high frequencies studied there is a significant departure

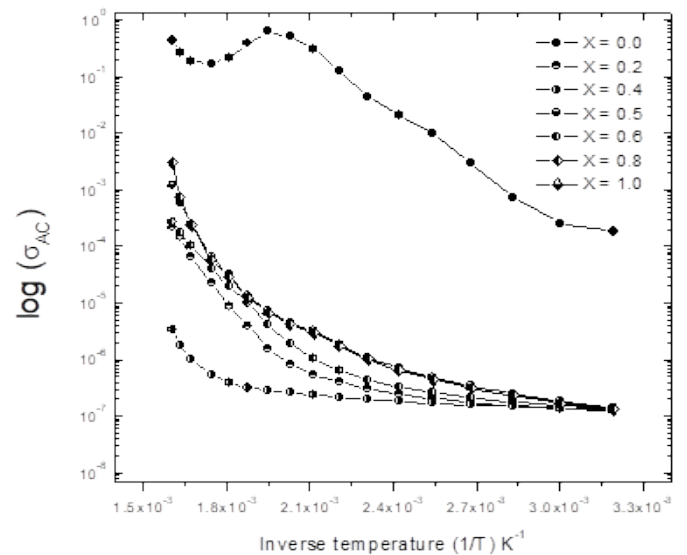


**Figure 6.** Temperature dependence of AC electrical conductivity  $\log(\sigma_{AC})$  temperature for NiCuZn- MgCuZn composite ferrites.

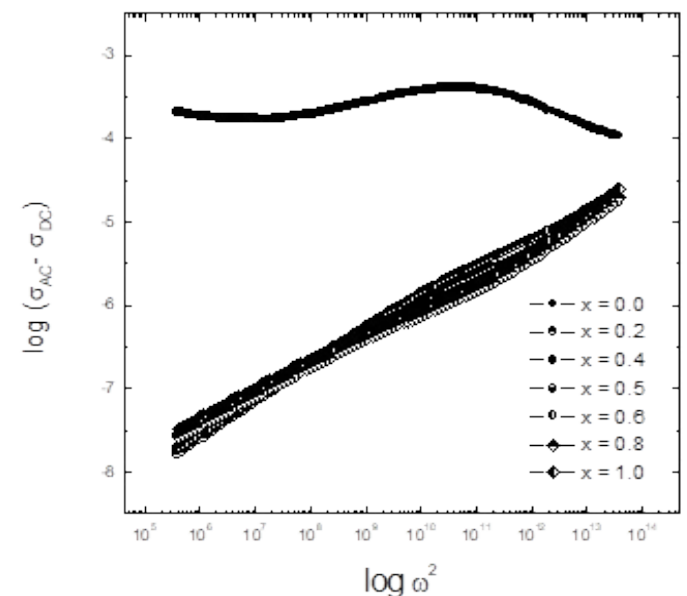


**Figure 7.** Variation of  $\log(\sigma_{AC} - \sigma_{DC})$  with  $\log \omega^2$  at room temperature for NiCuZn- MgCuZn composite ferrites.

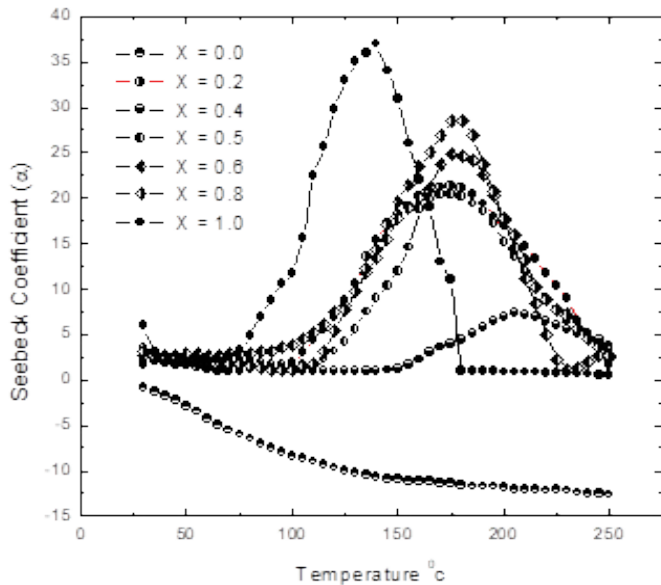


**Figure 8.** Temperature variation of Seebeck coefficient for NiCuZn-MgCuZn composite Ferrites.

from the linear relationship. At lower frequency, the grain boundaries are more active, hence the hopping frequency of electrons between  $\text{Fe}^{2+}$  and  $\text{Fe}^{3+}$  ions is less. So, the small Polaron hopping model is applicable only in the frequency region where the graphs show a linear relationship. At higher frequencies, the conductive grains become more active in promoting the hopping of electrons between  $\text{Fe}^{2+}$  and  $\text{Fe}^{3+}$  ions therefore increasing the hopping frequency [37].

Hence, it may be concluded that the conduction mechanism in these ferrites is due to mixed Polaron hopping. A similar type of behaviour was noticed [20] in the case of NiMgCuZn ferrites. As the linearity of the plots at lower frequency is attributed to small Polaron type conduction [38]. So we observed high resistivity value.

The room temperature values of the Seebeck coefficient are given in Table 2. It can be seen from Table 2 that the sign of the Seebeck coefficient at room temperature is negative only for  $X=0.0$ , while it is positive for all the other samples. This in conformity with literature data [39]. The Seebeck coefficient of these composite ferrites are graphically shown in Figure 8. It can be observed except for  $X=0.0$  the Seebeck coefficient for all the specimens shows kinks with increase in temperature. Hence, it can be inferred from these figures that due to addition of NiCuZn ferrite to MgCuZn ferrites cause the conduction process to change from N-type to P-type. Thus the conduction mechanism in these ferrites is predominantly due to hopping of charges [40] from  $\text{Fe}^{2+}$  to  $\text{Fe}^{3+}$  ions.



## Conclusions

The DC resistivity values of all ferrites composites are found to be  $10^9 \Omega\text{-cm}$  which meets the requirement of MLCIs. The variation of AC conductivity suggests that conduction is due to the conduction mechanism is found to be mixed Polaron hopping. The electrical properties of NiCuZn and MgCuZn composite ferrites showed high resistivity, So this would be better core material for the fabrication of multilayer chip inductors (MLCI).

## Acknowledgments

This work was financially supported by Defence Research and Development Organization (DRDO), under the grants ERIP/ER/0103301/M/01, New Delhi, India. The author is thankful to the authorities of Sri Krishnadevaraya University, Anantapur for providing the facilities.

## References

1. Neelakanta, Perambur S. "Handbook of electromagnetic materials: monolithic and composite versions and their applications." CRC press (1995).
2. Levinson, Lander. "Electronic Ceramics: Properties, Devices, and Applications." New York, NY: Marcel Dekker (1988).
3. Qi, Xiwei, Ji Zhou, Zhenxing Yue, and Zhilun Gui, et al. "A ferroelectric ferromagnetic composite material with significant permeability and permittivity." *Advanced Functional Materials* 14.9 (2004): 920-926.
4. Mudinepalli, Venkata Ramana, SH Song, M Ravi, and JQ Li, et al. "Multiferroic properties of lead-free  $\text{Ni}_0.5\text{Zn}_0.5\text{Fe}_{1.9}\text{O}_4-\delta-\text{Na}_0.5\text{Bi}_0.5\text{TiO}_3$  composites synthesized by spark plasma sintering." *Ceramics International* 41.5 (2015): 6882-6888.
5. Reddy, M. Penchal, W Madhuri, M Venkata Ramana, and IG Kim, et al. "Possibility of NiCuZn ferrites composition for stress sensor applications." *Journal of Ceramics* (2013).
6. Prasad, Arun S, Dolia SN, Dhawan MS, and Kumar S, et al. "Synthesis, Structural and Magnetic Properties of Polypyrrole Coated  $\text{Ni}_0.2\text{Ca}_0.8\text{Fe}_2\text{O}_4$  Nanocomposite." *Journal of Superconductivity and Novel Magnetism* 28.4 (2015): 1425-1425.
7. Qi, Xi Wei, Ji Zhou, Zhen Xing Yue, and Long Tu Li, et al. "Room temperature preparation of nanocrystalline MnCuZn ferrite powder by auto-combustion of nitrate-citrate gels." *Key Engineering Materials*. Vol. 224. Trans Tech Publications Ltd, 2002.
8. Qi, Xiwei, Ji Zhou, Zhenxing Yue, and Zhilun Gui, et al. "Effect of Mn substitution on the magnetic properties of MgCuZn ferrites." *Journal of Magnetism and Magnetic Materials* 251.3 (2002): 316-322.
9. Zhang, Hongguo, Zhenwei Ma, Ji Zhou, and Zhenxing Yue, et al. "Preparation and investigation of  $(\text{Ni}_0.15\text{Cu}_0.25\text{Zn}_0.60)\text{Fe}_{1.96}\text{O}_4$  ferrite with very high initial permeability from self-propagated powders." *Journal of magnetism and magnetic materials* 213.3 (2000): 304-308.
10. Nakamura, Tatsuya. "Low-temperature sintering of NiZnCu ferrite and its permeability spectra." *Journal of Magnetism and Magnetic Materials* 168.3 (1997): 285-291.
11. Jean, Jau-Ho, Cheng-Hong Lee, and Wen-Song Kou. "Effects of Lead (II) Oxide on Processing and Properties of Low-Temperature-Cofirable Ni-Cu-Zn Ferrite." *Journal of the American Ceramic Society* 82.2 (1999): 343-350.
12. Nakano, Atsuyuki, Isao Nakahata, and Taku Murase. "Electromagnetic Properties of Low Temperature Sintering MaCuZn Ferrites." *Journal of the Japan Society of Powder and Powder Metallurgy* 48.2 (2001): 131-135.
13. Rezlescu, N, Rezlescu E, Popa PD and Craus ML, et al. "Copper ions influence on the physical properties of a magnesium-zinc ferrite." *Journal of Magnetism and Magnetic Materials* 182.1-2 (1998): 199-206.
14. Rezlescu, N, Sachelarie L, Rezlescu L, and Popa PD. "Influence of PbO and Ta<sub>2</sub>O<sub>5</sub> on some physical properties of MgCuZn ferrites." *Crystal Research and Technology: Journal of Experimental and Industrial Crystallography* 36.2 (2001): 157-167.
15. Sachelarie, L, Rezlescu E, and Rezlescu N. "Influence of PbO on some properties of MgCuZn ferrites." *physica status solidi (a)* 179.1 (2000): R1-R3.
16. Bhosale, DN, Choudhari ND, Sawant SR, and Bakare PP. "Initial permeability studies on high density Cu Mg Zn ferrites." *Journal of Magnetism and Magnetic Materials* 173 (1997): 51-58.
17. Varalaxmi, Narla, N. Ramamanohar Reddy, Mudinepalli Venkata Ramana, and Eyunni Rajagopal, et al. "Stress sensitivity of inductance in NiMgCuZn ferrites and development of a stress insensitive ferrite composition for microinductors." *Journal of Materials Science: Materials in Electronics* 19.5 (2008): 399-405.
18. Varalaxmi, Narla. "High permeability and stress insensitivity of MgCuZn-NiCuZn ferrite composites for microinductor applications." *Journal of Materials Science: Materials in Electronics* 22.5 (2011): 555-560.
19. Murthy, VRK and Sobhanadri J. "Electrical conductivity of some nickel-zinc ferrites." *physica status solidi (a)* 38.2 (1976): 647-651.
20. Varalaxmi, Narla, and Sivakumar KV. "Studies on AC and DC electrical

- conductivity and thermo-electric power of NiMgCuZn ferrites." *International Journal of Nanoparticles* 3.4 (2010): 349-366.
21. Reddy, V Devender, Malik MA, and Venugopal Reddy P. "Electrical transport properties of manganese-magnesium mixed ferrites." *Materials Science and Engineering: B* 8.4 (1991): 295-301.
  22. Wolska, E, Riedel E, and Wolski W. "The Evidence of Cd<sup>2+</sup> xFe [Ni Fe] O<sub>4</sub> Cation Distribution Based on X-Ray and Mössbauer Data." *physica status solidi (a)* 132.1 (1992): K51-K56.
  23. Červinka, L, and Šimša Z. "Distribution of copper ions in some copper-manganese ferrites." *Czechoslovak Journal of Physics B* 20 (1970): 470-474.
  24. Ladgaonkar, BP, and Vaingankar AS. "X-ray diffraction investigation of cation distribution in Cd<sub>x</sub>Cu<sub>1-x</sub>Fe<sub>2</sub>O<sub>4</sub> ferrite system." *Materials Chemistry and Physics* 56.3 (1998): 280-283.
  25. Madhuri, W, Reddy MP, Kim IG, and Reddy NRM, et al. "Transport properties of microwave sintered pure and glass added MgCuZn ferrites." *Materials Science and Engineering: B* 178.12 (2013): 843-850.
  26. Cullity, Bernard Dennis. *Elements of X-ray Diffraction*. Addison-Wesley Publishing (1956).
  27. Smit J, and Wijn HPJ. "Physical Properties of ferromagnetic Oxide in relation their Technical Properties" *Philips Technical Library* 163 (1959):143
  28. Hodgmann, CD. "Handbook of Chemistry and Physics 36<sup>th</sup> Edn." Chemical Rubber Co: Cleveland OH, (1954-55):3095-3097.
  29. Snelling, EC. "Soft Ferrites." 2nd edn., Butterworths, London (1998).
  30. Shrotri, JJ, Kulkarni SD, Deshpande CE, Dtate SK. "Effect of Cu substitution on the magnetic and electrical properties of Ni-Zn ferrite synthesised by soft chemical method." *Materials chemistry and physics* 59.1 (1999): 1-5.
  31. Nakamura T. "Low-temperature sintering of NiCuZn ferrites and its permeability spectra." *J Magn Magn Mater*. 168 (1997): 285-289.
  32. Yue, Zhenxing, Ji Zhou, Longtu Li, and Xiaohui Wang, et al. "Effect of copper on the electromagnetic properties of Mg-Zn-Cu ferrites prepared by sol-gel auto combustion method." *Mater Sci and Eng B* 86 (2001): 64-69.
  33. Karche, BR, Khasbardar BV, and Vaingankar AS. "X-ray, SEM and magnetic properties of MgCd ferrites." *J Magn Magn Mater*. 168 (1997): 292-298.
  34. Tsay, CY, Liu KS, Lin TF, and Lin IN. "Microwave sintering of NiCuZn ferrites and multilayer chip inductors." *J Magn Magn Mater* 209 (2000):189-192.
  35. Gul, IH, Ahmed W, and Maqsood A. "Electrical and magnetic characterization of nano crystalline Ni-Zn ferrite synthesis by co-precipitation route." *J Magn Magn Mater*. 320 (2008):270-275.
  36. Van Uiter LG. "Proc IRE." (1956): 1294.
  37. Sindhu, S, Anantharaman MR, Thampi BP, and Malni KA, et al. "Evaluation of a.c. conductivity of rubber ferrite composites from dielectric measurements." *Bull Mater Sci*. 25 (2002): 599-607.
  38. Alder, Alber, feinleib Jabner. "Electrical and Optical Properties of Narrow-Band Materials." *Phys Rev B* 2 (1970): 3112-3134.
  39. Viswanathan, B and Murthy VRK. "Ferrites - Science and Technology Springer-Verlag." Narosa Publishing House (1990): 37.
  40. VanUiter, LG. "DC Resistivity in the Nickel and Nickel Zinc Ferrite System." *J Chem Phys* 23 (1955):1883-1887.

**How to cite this article:** Varalaxmi N. "The Possibility of Utilizing the Composite Ferrites as Core Material for the Fabrication of Multilayer Chip Inductors (MLCI)". *J Material Sci Eng* 9 (2020) doi: 10.37421/jme.2020.9.553